Chapter 2
Ballistic Impact Experiments and Quantitative Assessments of Mesoscale Damage Modes in a Single-Layer Woven Composite

Christopher S. Meyer, Enock Bonyi, Bazle Z. Haque, Daniel J. O'Brien, Kadir Aslan, and John W. Gillespie Jr

Abstract In this work, we investigated the mesoscale impact and perforation damage of a single layer, woven composite target transversely impacted below and above the ballistic limit by a rigid projectile sized on the order of a tow width. To visualize mesoscale impact damage in woven composites, a thin translucent composite target was used, which provided access to both impact and back-face surfaces. High-resolution photography was used to visualize mesoscale damage, and impact and residual velocity data relative to the location of projectile impact on weaving architecture were quantified. It was found that impact on a tow-tow crossover requires more energy to perforate than impact on a matrix-rich interstitial site or on adjacent, parallel tows. Mesoscale damage in thin, woven composites was characterized for impact velocities below and above the ballistic limit. Four mesoscale damage modes were identified: transverse tow cracks, tow-tow delamination, 45° matrix cracks, and punch- shear. These damage modes were observed both on the surface and inside the composites. High-resolution images of these damage modes were quantified in digital damage maps whereby the output of color intensity correlated with the quantity and type of material damage. Digital maps generated for select specimens revealed characteristic damage patterns in woven fabric composites including a diamond pattern in matrix cracking and a cross pattern in tow–tow delamination. It was found that the greatest extent and quantity of mesoscale damage occurs for impact velocity just below the ballistic limit.

Keywords Transverse crack · Delamination · Mesoscale · Damage · Impact

2.1 Introduction

Length scales associated with the weaving architecture of woven fabric composite materials play an important role in the energy dissipation mechanisms of composites. "Macroscale" is the structural length scale of composites, "mesoscale" is the fiber-tow or yarn length scale of woven composites, and "microscale" is the fiber length scale of composites. Under transverse ballistic impact, the weaving architecture provides additional energy dissipation mechanisms over laminated, unidirectional composites. Kinetic energy of projectiles impacting fiber reinforced polymer composites is dissipated through macroscale damage modes and microscale damage mechanisms. Energy dissipating macroscale damage modes include crush, punch-shear, compression-shear, tension-shear, transverse tow damage and delamination, and in-plane matrix damage. Energy dissipating microscale damage mechanisms include fiber fracture, fiber-matrix interface debonding, matrix cracking, and frictional sliding. The weaving architecture of textile composites provides mesoscale energy dissipation mechanisms including primary tow matrix cracking, tension-shear and compression-shear tow failure, elastic deformation of secondary tows [1], additional delamination resistance due to the out-of-plane undulation [2], tow-tow and tow-matrix delamination [3], and coupled tension and bending due to local undulation of interwoven tows [4]. Impact kinetic energy is dissipated at the

C. S. Meyer (✉)
University of Delaware, Center for Composite Materials, Newark, DE, USA

US Army Research Laboratory, Aberdeen Proving Ground, Aberdeen, MD, USA
e-mail: csmeyer@udel.edu

E. Bonyi · K. Aslan
Morgan State University, Department of Civil Engineering, Baltimore, MD, USA

B. Z. Haque · J. W. Gillespie Jr
University of Delaware, Center for Composite Materials, Newark, DE, USA

D. J. O'Brien
US Army Research Laboratory, Aberdeen Proving Ground, Aberdeen, MD, USA

J. Kimberley et al. (eds.), *Dynamic Behavior of Materials, Volume 1*, Conference Proceedings of the Society for Experimental Mechanics Series, https://doi.org/10.1007/978-3-319-95089-1_2

mesoscale in woven composites by mesoscale damage modes: transverse tow cracking, tow-tow delamination, 45° matrix cracking, and punch-shear damage [5, 6]. Mesoscale damage modes are comprised of microscale damage mechanisms. Thus, mesoscale energy dissipation and damage come from the accumulation of energy dissipating microscale damage mechanisms.

Impactor dimension relative to the composite is another important length scale, and the impactor nose shape influences how kinetic energy is transmitted into the composite. Mesoscale damage modes and mechanisms occur at the length scale of the individual tows so impactor diameter on the order of tow width may influence the macroscopic damage modes such as punch-shear and crush. A projectile diameter less than the fabric tow width may impact on individual tows, tow-tow crossovers, and interstitial resin pockets; however, larger diameter projectiles will impact on multiple tows. A mesoscale impact model considering projectile diameter is necessary to understand the effect of weaving architecture on the impact damage behavior of woven fabric composites [5].

Thickness of the composite is another length scale that must be considered in the study of impact damage modes and mechanisms. In previous works, Haque et al. [7–9] studied and modeled the ballistic impact response of different composite laminates. In those works, the ballistic impact is described with three phenomenologically different phases: (1) penetration; (2) transition; and (3) perforation. Each of these phases is dominated by different deformation and damage mechanisms. During the penetration phase, there is little deformation in the material ahead of the projectile up to the target back face. Penetration is dominated by through-thickness compression, fiber crush, fiber-matrix shear, and material flow from the annulus surrounding the projectile-target contact region. As the impact event enters the transition phase, the material surrounding and ahead of the projectile begins to experience transverse shear deformation resulting in delamination and the appearance of a "deformation cone" ahead of the projectile moving at a slower velocity than the projectile. In the perforation phase, the projectile and target move at the same relative velocity, and deformation is dominated by compression-shear ahead of the projectile and in-plane tension-shear around the projectile.

The extent to which any given target exhibits each of the three phases of penetration, transition, and perforation is determined by the relative target and projectile geometries. Very thick laminates are dominated by penetration while very thin targets are dominated by perforation. For penetration mechanics of composite materials, a thick composite is herein defined as one in which penetration, transition, and perforation occurs; a thin composite is defined as one in which only perforation occurs. An intermediate thickness composite (between thick and thin) can be defined which shows little or no penetration but shows both the transition and perforation phases. Perforation damage mechanisms can be isolated by ballistic testing of a thin composite laminate, and in the limit, by testing a single layer woven fabric composite laminate. Lomov et al. [4] noted that single-ply composites are seldom tested (or used), but local variations due to lamina nesting, random tow placement, and interpenetration and overlapping of tows in multi-layer composites contributes to error in strain field characterization. The work by Lomov et al. [4] suggests that experiments on a single ply can provide insight into the material behavior by minimizing sources of error related to the interaction between multiple plies.

Impact kinetic energy is another important consideration in composite impact and damage, so projectile impact on composite targets must also consider impact velocity as an important variable. The ballistic limit velocity of a projectile-target pair, V_{BL}, is a function of target material properties, thickness, and weaving architecture, and of projectile mass, length and diameter, and nose shape. Ballistic limit velocity is related to and sometimes called V_{50}, which is a statistical measure defined as the projectile impact velocity for which at least 50% of ballistic impacts perforate the target and the remainder rebound or lodge in the target [10].

The theories of transverse impact on a 1D fiber [11–16] and a 2D membrane [17] provide important insight into the perforation mechanics of a single layer, thin composite plate. When a projectile transversely impacts a thin composite target, an implosion wave (axial stress wave) travels outward from the projectile impact location, and a transverse deformation cone develops such that the edge or kink point of the cone propagates out from the point of impact, satisfying the conservation of momentum and energy. The transverse deformation cone propagates with a cone wave-front velocity that depends on the axial wave speed of the target material and the projectile impact velocity. The implosion or axial wave speed of the target depends only on the target material properties. The mechanism of momentum and energy transfer to the target depends on the implosion wave speed and the cone wave speed. With increasing projectile impact velocity, the rate of momentum and energy transfer to the target increases. As the impact velocity increases to the ballistic limit velocity, the total momentum of the projectile is transferred to the target. Impact velocities greater than the ballistic limit exceed the composite target's capacity to dissipate energy without catastrophic failure in the neighborhood of the projectile, so the projectile perforates and exits the target with some residual velocity in the direction of impact.

All transverse impacts of composite materials with projectile velocities exceeding the ballistic limit include the perforation phase, regardless of composite thickness. Therefore, understanding ballistic impact damage necessitates studying the perforation phase. To isolate and examine the damage modes and mechanisms present in the perforation phase up to and exceeding the ballistic limit velocity, the present study examined a composite plate made from a single ply of woven S-2

Table 2.1 Average S-2 glass/SC-15 composite properties

Density	$\rho_C^{avg} = 1.758 \pm 0.03$	g/cm^3
Thickness	$H_C = 0.887 \pm 0.024$	mm
Areal density	$AD = \rho_C H_C = 1.559$	kg/m^2

glass fiber. A single ply composite ensures that neither the penetration nor transition phases will be present, but only the perforation phase will occur. To investigate the perforation dominated mesoscale damage modes and mechanisms associated with thin woven fabric composites, ballistic impact experiments were conducted with a 5.6 mm (.22 caliber) right circular cylindrical steel projectile impacting a single layer, plain-weave S-2 Glass/SC15 composite. To investigate kinetic energy, momentum transfer, and mesoscale damage, impact velocities up to and exceeding the ballistic limit velocity were recorded, impact locations relative to tow-tow crossovers were determined, and mesoscale damage was characterized and quantified using high-resolution optical photography.

2.2 Experimental Setup

Vacuum-assisted resin transfer molding was used to produce single-ply composite panels from plain-weave (PW) S-2 glass fabric (5×5 tows/inch, areal density of one ply is 744 g/m^2 (24 oz./yd^2), AGY 463-AA-2BL, 30 ends) infused with SC15 epoxy resin (Applied Poleramic, Benicia, CA). A two-part cure under vacuum was followed, first at 35 °C (95 °F) for 24 h and then temperature ramped up at 0.5 °C/min to 115 °C (239 °F) and was held for 3 h. A wet saw was used to machine ballistic test specimens that were 304 mm × 304 mm (12 inch × 12 inch) in-plane dimensions. Properties of the composite are provided in Table 2.1. A smooth bore, helium gas gun was used to propel steel right circular cylindrical projectiles into the fixtured targets. The fixture clamped the targets between two 360 mm square by 6.4 mm thick aluminum plates with 203 mm (8 inch) diameter central holes. Impact and residual velocity were measured by radar. Mechanical properties of the composites may be found in a prior publication [5]. Post-experimental high-resolution images were captured using a Phase One IQ180 80 MP CCD digital back and DT RCam reprographic camera, Phase One 120 mm macro lens, Kaiser RSD adjustable copy stand, and Huion light box backlight and two movable incandescent front lights. The full resolution of these images is 10,328 x 7760 pixels and a spatial resolution of 300 dots per inch. The smallest size that can be resolved is 84 μm, sufficient to distinguish multiple transverse cracks across an average 5080 μm tow width. Image resolution allowed ImageJ [18] processing to correlate projectile impact location to either a "center impact (A)" on fiber-rich tow-tow crossovers or an "off-center impact (B)" on adjacent parallel tows or matrix-rich interstitial regions within the PW architecture. High-resolution images were inspected and damage was counted and translated into digital damage maps with MATLAB.

2.3 Ballistic Results

Impact velocity, V_I, and residual velocity, V_R, are provided in Table 2.2, along with the relative impact locations, either "center impact (A)" or "off-center impact (B)." Ballistic limit velocity was calculated for center impact ($V_{50}^A = 188$ m/s), but there was insufficient data for calculating ballistic limit velocity for off-center impact (V_{50}^B) in accordance with MIL-STD-662F [10]. Hence, the ballistic limit equations by Lambert and Jonas [19] and Haque and Gillespie [20] were used to fit the data and determine a ballistic limit velocity for center impact $V_{BL,LJ}^A = 188$ m/s, $V_{BL,HG}^A = 187$ m/s and off-center impact $V_{BL,LJ}^B = 167$ m/s, $V_{BL,HG}^B = 166$ m/s. These data and fits are plotted in Fig. 2.1a for center impact and in Fig. 2.1b for off-center impact. Since the targets were thin, single-layer composites projectiles either perforated or rebounded, so the data in Fig. 2.1 is separated into complete perforation or no perforation.

2.4 Quantitative Investigation of Mesoscale Damage

Damage mechanisms were investigated for impact velocities close to the ballistic limit using high-resolution images for a non-perforation at an impact velocity slightly less than the ballistic limit velocity, target 5158–22, $V_I = 162$ m/s, $V_R = -26$ m/s, shown in Fig. 2.2, and for a complete perforation at an impact velocity a slightly more than the ballistic

Table 2.2 Perforation data of single layer PW S-2 Glass/SC-15 composites, for center impact, A, and off-center impact, B

Target ID	Impact velocity V_I, *m/s*	Residual velocity V_R, *m/s*	Relative impact locations
5159–1	104	−14	B
5159–2	125	−19	A
5159–3	166	−25	A
5159–4	214	134	A
5159–5	293	257	B
5159–6	200	129	A
5159–7	188	−25	A
5159–8	198	113	B
5159–9	186	121	B
5159–10	153	−24	A
5159–11	488	N/A	N/A
5159–12	472	448	B
5159–13	439	412	A
5159–14	355	322	A
5159–15	239	191	A
5155–16	195	137	B
5155–17	186	119	B
5159–18	177	−32	A
5155–19	181	102	A
5155–20	174	62	B
5155–21	167	84	B
5158–22	162	−26	A
5158–23	166	−26	A
5158–24	215	175	B
5155–25	282	254	B
5158–6	173	−97	A
5155–10	152	N/A	A

limit velocity, target 5155–17, $V_I = 186$ m/s, $V_R = 119$ m/s, shown in Fig. 2.3. White lines mark approximate tow widths and interstitial, matrix-rich areas between fiber tows in Figs. 2.2 and 2.3. Transverse tow cracking, tow-tow delamination, and 45° matrix cracking are damage modes that occur in the mesoscale [5, 6], the scale of a tow-width, as seen in Figs. 2.2 and 2.3. In ballistic impact, transverse cracks initiate and propagate due to primary tow [21] in-plane tensile loading, which is spread by in-plane shear. Shear lag redistributes this loading as transverse cracks form, leading to formation of multiple, roughly parallel transverse cracks across tow widths, as seen in Figs. 2.2 and 2.3. Transverse cracks propagate parallel to the fiber direction and may spread across multiple unit cells, as seen in Figs. 2.2 and 2.3. Transverse cracks propagate through the tow thickness until intersecting orthogonal tows, then the cracks turn and propagate between orthogonal tows becoming tow-tow delamination. Accumulation of transverse cracks reduces the composites capacity for spreading load by in-plane shear and causes primary tows to be loaded preferentially. Primary tows stretch in tension and form an expanding pyramid of deformation, and in-plane shear and bending at the expanding pyramid wave-front lead to progressively larger diamonds of 45° matrix cracks in matrix-rich interstitial regions, as may be seen in Figs. 2.2 and 2.3. Sufficiently energetic impacts cause punch-shear damage as the projectile punches through the composite, causing tension-shear fracture of fibers and matrix around the projectile annulus, fiber-matrix interface debonding, and matrix pulverization and ejection. The reader is referred to other works by the authors for additional discussion on these mesoscale damage modes [5, 6].

2.5 Qualitative Investigation of Mesoscale Damage

The high-resolution images captured for several specimens had their mesoscale damage modes quantified. The images were inspected for transverse cracks, tow-tow delamination, and 45° matrix cracks, and the quantity of each damage mode was counted for each unit cell in a 41x41 grid of unit cells across the 203 mm (8 inch) diameter (each unit cell is 5.08 mm square). The quantities of each damage mode were placed into damage maps to provide at-a-glance visual representations of

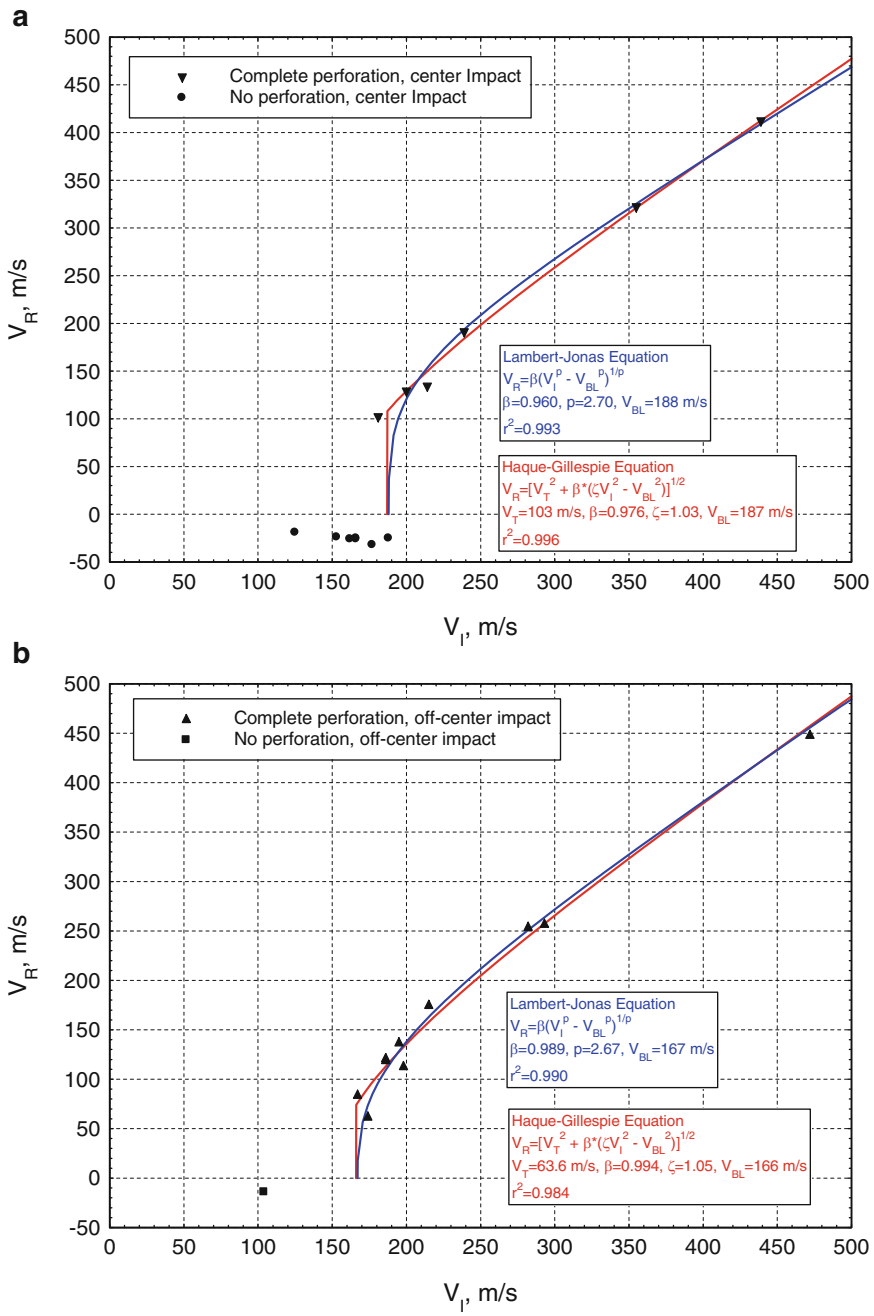

Fig. 2.1 Ballistic limit analysis of perforation data presented in Table 2.1 with determination of V_{BL} for (**a**) center impact and for (**b**) off-center impact using Lambert-Jonas [19] and Haque-Gillespie [20] ballistic limit equations

the damage modes. Fig. 2.4 provides damage maps for (a) transverse cracks, (b) tow-tow delamination, and (c) 45° matrix cracks. In Fig. 2.4, color bars are provided such that the color intensity in the figure can give the viewer an at-a-glance visual estimate of the quantity of each damage type. In this way, it is seen that damage increases up to a maximum at the ballistic limit and decreases thereafter as the damage occurs under higher energy density. The front face damage is quantified in Table 2.3. In Table 2.3, tow-tow delamination total represents total number of unit cells with any percentage of delamination, while other damage totals are actual numbers of cracks counted per unit cell and totaled across the specimen.

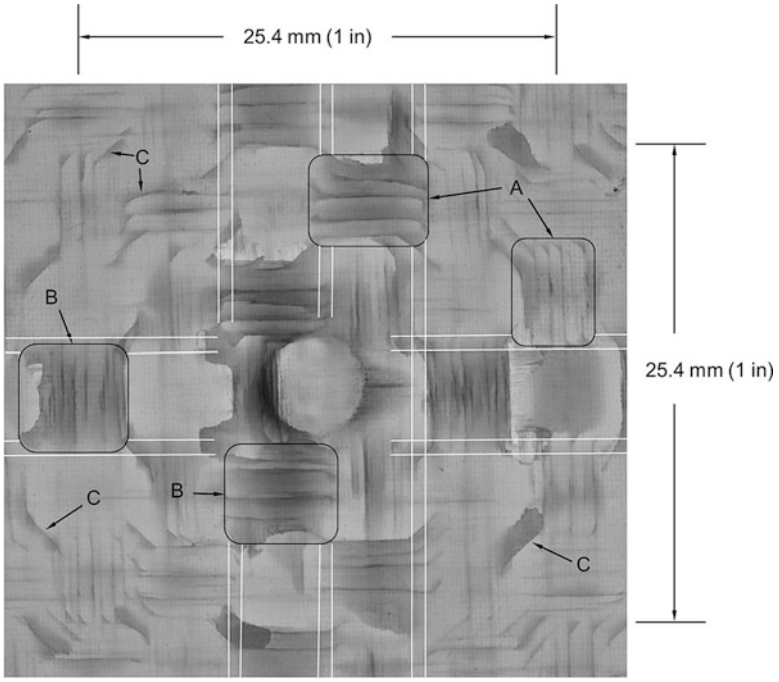

Fig. 2.2 Damage mechanisms in an off-center impact, non-perforated target, 5158–22, $V_I = 162$ m/s, $V_R = -26$ m/s with (**a**) transverse tow cracking, (**b**) tow-tow delamination, and (**c**) 45° matrix cracking primary tows and interstitial matrix-rich areas between woven tows indicated by white lines

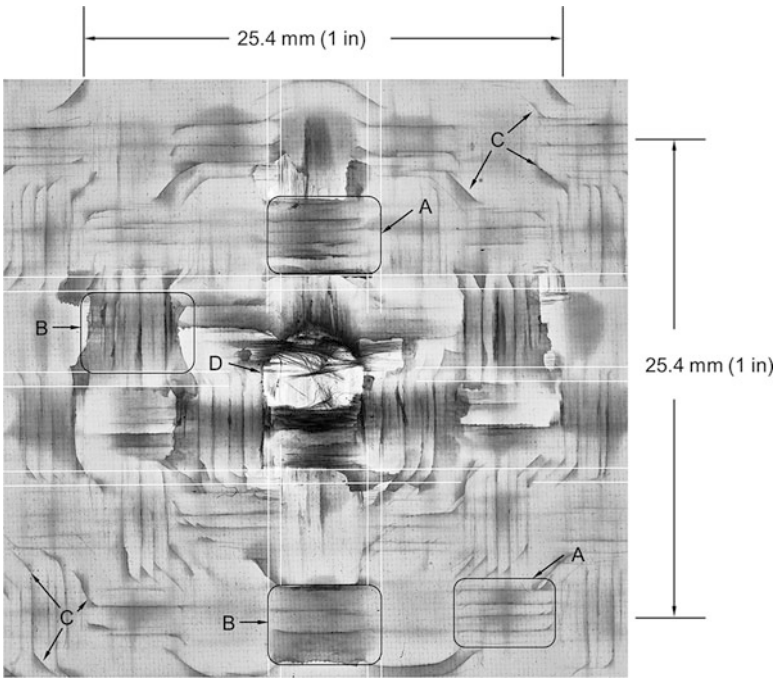

Fig. 2.3 Damage mechanisms in an off-center impact, completely-perforated target 5155–17, $V_I = 186$ m/s, $V_R = 119$ m/s with (**a**) transverse tow cracking, (**b**) tow-tow delamination, (**c**) 45° matrix cracking, and (**d**) punch-shear damage and interstitial matrix-rich areas between woven tows indicated by white lines

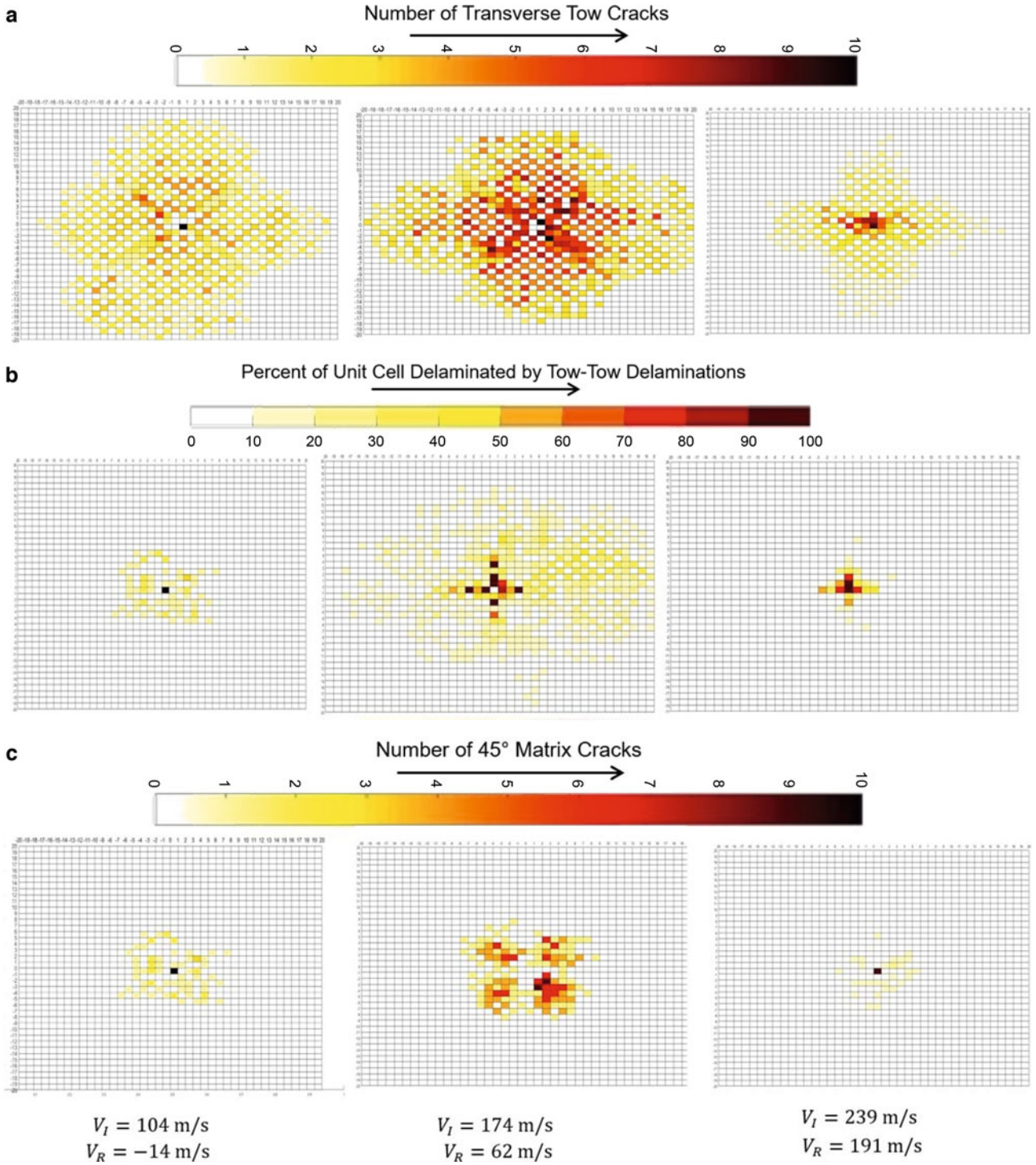

Fig. 2.4 Digital damage maps of (**a**) transverse cracks, (**b**) tow-tow delamination, and (**c**) 45° matrix cracks for three impact velocities, one less than (Left, $V_I = 104$ m/s), one near to (Middle, $V_I = 174$ m/s), and one greater than (Right, $V_I = 239$ m/s) the ballistic limit velocity

2.6 Conclusions

Ballistic impact experiments were conducted on a single-layer woven composite with a projectile scaled on the order of a single tow width. Mesoscale damage modes occur at the length scale of a single tow width and these damage modes include transverse cracks, tow-tow delamination, and 45° matrix cracks. Distinct ballistic limit velocities were found for

Table 2.3 Damage quantification: total numbers of cracks, total number of delaminated unit cells, and percentages of area with each damage type

	Transverse cracks		45° Matrix cracks		Tow-tow delamination	
Target ID	Total	% of area damaged	Total	% of area damaged	Total	% of area damaged
5159–1	953	28.3	71	3.5	287	17.1
5159–10	1236	34.6	378	15.9	57	15.3
5155–20	1302	31.3	204	7.7	802	47.7
5159–8	1252	31.3	247	8.7	302	18.0
5159–15	541	13.3	105	4.5	77	4.6
5155–25	346	7.9	58	2.5	61	3.6
5159–14	529	13.3	78	3.7	79	4.7
5159–12	279	7.6	28	1.5	51	3.0

two different impact locations indicating, as expected, greater energy is required to perforate at the fiber-rich tow overlaps and less energy is required to perforate fiber-poor and matrix-rich interstitial regions. This result is expected because of the differences in strength and load distribution, hence differences in damage evolution and energy dissipation, between these two impact locations. This mesoscale effect would not be seen for projectiles scaled larger than a tow width since the energy is distributed over a wider area and dissipation is averaged over these distinct fiber-rich and matrix-rich regions. Three mesoscale damage modes were qualitatively investigated using high-resolution optical inspection of a back-lit, thin, translucent plain weave glass fiber reinforced epoxy composite. These three mesoscale damage modes were also quantified using high-resolution imaging and were graphically depicted in damage maps to provide at-a-glance visual identification of this damage. From these damage maps, it was found that the extent of damage increases with increasing impact velocity and is a maximum at the ballistic limit velocity, and the extent of damage then decreases for impact velocities beyond the ballistic limit. Inspection of damage maps also reveals that tow-tow delamination is concentrated in primary tows and nearby secondary tows, as revealed by the cross-pattern of tow-tow delamination. Inspection of damage maps also reveals that 45° matrix cracks are concentrated in quadrants separated by the cross of primary tows. These ballistic impact data, high-resolution qualification and quantification of mesoscale damage, and digital damage maps provide useful data for gleaning new understanding of the time-resolved process of damage evolution in perforation of thin composites and are useful for finite element model validation.

Acknowledgements Research was sponsored by the U.S. Army Research Laboratory and was accomplished under Cooperative Agreement Number W911NF-12-2-0022. The views and conclusions contained in this document are those of the authors and should not be interpreted as representing the official policies, either expressed or implied, of the U.S. Army Research Laboratory or the U.S. Government. Thanks to Molla Ali of University of Delaware, Center for Composite Materials for help with material characterization. Thanks to Zuhal Onuk, Bridgit Kioko, Oreoluwa Adesina, and Carisse Lansiquot of Morgan State University for help with MATLAB scripting and damage counting. Thanks to Nebiyou Getinet and Jian Yu of the U.S. Army Research Laboratory for help with conducting ballistic experiments.

References

1. Gower, H.L., Cronin, D.S., Plumtree, A.: Ballistic impact response of laminated composite panels. Int. J. Impact Eng. **35**, 1000–1008 (2008)
2. Karkkainen, R.L.: Dynamic micromechanical modeling of textile composite strength under impact and multi-axial loading. Compos. Part B Eng. **83**, 27–35 (2015)
3. Karkkainen, R.L., Mcwilliams, B.: Dynamic micromechanical modeling of textile composites with cohesive interface failure. J. Compos. Mater. **46**(18), 2203–2218 (2012)
4. Lomov, S.V., et al.: Full-field strain measurements for validation of meso-FE analysis of textile composites. Compos. Part A Appl. Sci. Manuf. **39**(8), 1218–1231 (2008)
5. Meyer, C.S., et al.: Mesoscale ballistic damage mechanisms of a single-layer woven glass/epoxy composite. Int. J. Impact Eng. **113**(November 2017), 118–131 (2018)
6. Bonyi, E., et al.: Assessment and quantification of ballistic impact damage of a single-layer woven fabric composite. Int. J. Damage Mech. (2018)
7. Gama, B.A., Gillespie, J.W.: Finite Element Modeling of Impact, Damage Evolution and Penetration of Thick-Section Composites. Int. J. Impact Eng. **38**, 181–197 (2011)
8. Haque, B.Z., Gillespie Jr., J.W.: Penetration and Perforation of Composite Structures. Mech. Eng. Res. J. **9**(March), 37–42 (2013)
9. Jordan, J.B., Naito, C.J., Haque, B.Z.: Progressive damage modeling of plain weave E-glass/phenolic composites. Compos. Part B Eng. **61**, 315–323 (2014)
10. Military Test Method Standard MIL-STD-662F, V50 Ballistic Test for Armor, *DOD*, 1997

11. Rakhmatulin, K.H.A.: Oblique impact at a large velocity on a flexible fiber in the presence of friction (in Russian). Prikl Mat Mekh. **9**, 449–462 (1945)
12. Rakhmatulin, K.H.A.: Impact on a flexible fiber (in Russian). Prikl Mat Mekh. **11**, 379–382 (1947)
13. Rakhmatulin, K.H.A.: Normal impact at a varying velocity on a flexible fiber (in Russian). Uchenye Zap. Moskovosk gos Univ. **4**, 154 (1951)
14. Rakhmatulin, K.H.A.: Normal impact on a flexible fiber by a body of given shape (in Russian). Prikl Mat Mekh. **16**, 23–24 (1952)
15. Smith, J.C., McCracking, F.L., Schiefer, H.F.: Stress-strain relationships in yarns subjected to rapid impact loading. Part V: wave propagation in long textile yarns impacted transversely. J. Res. Natl. Bur. Stand. (1934). **60**(5), 701–708 (1955)
16. Smith, J.C., McCrackin, F.L., Schiefer, H.F.: Stress-strain relationships in yarns subjected. Text. Res. J. **28**, 288–302 (1958)
17. Leigh Phoenix, S., Porwal, P.K.: A new membrane model for the ballistic impact response and V50performance of multi-ply fibrous systems. Int. J. Solids Struct. **40**(24), 6723–6765 (2003)
18. Schneider, C.A., Rasband, W.S., Eliceiri, K.W.: NIH image to ImageJ: 25 years of image analysis. Nat. Methods. **9**(7), 671–675 (2012)
19. Lambert, J.P., Jonas, G.H.: Towards standardization in terminal ballistics testing: velocity representation. BRL-R-1852, Aberdeen Proving Ground, MD (1976)
20. Haque, B.Z., Gillespie, J.W.: A new penetration equation for ballistic limit analysis. J. Thermoplast. Compos. Mater. **28**(7), 950–972 (2015)
21. Naik, N.K., Shrirao, P.: Composite structures under ballistic impact. Compos. Struct. **66**, 579–590 (2004)